AIP | The Journal of Chemical Physics

Dissociative adsorption of pyrrole on Si (111)-(7×7)

Ze Liang Yuan, Xian Feng Chen, Zhong Hai Wang, Kian Soon Yong, Yong Cao, and Guo Qin Xu

Dissociative adsorption of pyrrole on Si(111)-(7×7)

Ze Liang Yuan, Xian Feng Chen, Zhong Hai Wang, and Kian Soon Yong
Department of Chemistry, National University of Singapore, 10 Kent Ridge, Singapore, 119260

Yong Cao
Shanghai Key Laboratory of Molecular Catalysis and Innovative Materials, Department of Chemistry, Fudan University, Shanghai, 200433, People's Republic of China

Guo Qin Xu[a)]
Department of Chemistry, National University of Singapore, 10 Kent Ridge, Singapore, 119260

Pyrrole adsorption on Si(111)-(7×7) has been investigated using high-resolution electron energy loss spectroscopy (HREELS), thermal desorption spectroscopy, scanning tunneling microscopy (STM), and theoretical calculations. Compared to physisorbed pyrrole, chemisorption leads to the appearance of N–Si and Si–H vibrational features, together with the absence of N–H stretching mode. This clearly demonstrates the dissociative nature of pyrrole chemically binding on Si(111)-(7×7) through the breakage of N–H bond. Based on STM results, the resulting fragments of pyrrolyl and H atom are proposed to bind with an adatom and an adjacent rest atom, respectively. The STM images further reveal that the adsorption is site selective. The faulted center adatoms are most favored, followed by unfaulted center adatoms, faulted corner adatoms, and unfaulted corner adatoms. In addition, the chainlike pattern of reacted adatoms was observed, implying the possible existence of attractive interaction between adsorbed pyrrolyl and the precursor state. Theoretical calculation confirms that the dissociative adsorption with pyrrolyl bonded to an adatom and H atom to an adjacent rest atom is energetically favored compared to the associative cycloaddition involving the two α-carbon atoms of pyrrole and an adatom–rest atom pair. © *2003 American Institute of Physics.* [DOI: 10.1063/1.1619941]

I. INTRODUCTION

Due to its poisonous effects for metal catalysts used in petrochemical industry and exhaust gas conversion, the interaction of pyrrole with metal surfaces, such as Pd(111),[1,2] Rh(111),[3] Ni(100),[4] Cu(100),[5] and Pt(111)[6] was extensively studied. At low temperatures (ca. 200 K), pyrrole adsorbs molecularly with a flat-lying geometry, via π bonding with surfaces. Increasing the surface coverage leads to the change of its ring orientation from flat-lying to tilting towards the surface normal on Cu(100) and the upright on Pt(111) with nitrogen atom down. At elevated temperatures, pyrrole undergoes N–H bond cleavage, forming a tilted pyrrolyl radical (C_4H_4N) on Pd(111) and Rh(111) surfaces.

On the other hand, the binding of organic molecules on silicon surfaces has its potential application in microelectronics and device fabrication.[7–17] Compared to metal surfaces, Si(111)-(7×7) exhibits a diversity of reactive sites and is expected to have a rich surface chemistry. In one unit cell, there are various Si atoms with dangling bonds (dbs), including adatoms in the first layer, rest atoms in the second layer, and corner holes in the fourth layer. This great variety allows us to correlate the local environment of the surface sites with their reactivity.

The recent experimental and theoretical studies on adsorption of five-membered heterocyclic molecules, such as thiophene and furan, on Si(111)-(7×7) clearly demonstrated a cycloaddition reaction mechanism of thiophene and furan through its α–C atoms with the adjacent adatom and rest atom pair on Si(111)-(7×7) surfaces.[18,19] In addition to the cycloaddition, a dimerization reaction was also observed for furan on Si(111)-(7×7), suggesting a stepwise diradical mechanism.[19] On the other hand, the cleaved Si(111)-(2×1) surface was found to have a higher reactivity, facilitating thiophene and furan decomposition through desulfuration and deoxygenation processes, respectively.[15]

One of the important five-membered heterocyclic molecules is pyrrole, which was employed as a precursor for the synthesis of conducting polymers with valuable technological properties.[20] In addition, the covalently linked silicon/polypyrrole junctions were demonstrated to exhibit diode-like properties.[21,22] In this work, we present the adsorption configuration of pyrrole on Si(111)-(7×7) concluded from the HREELS, TDS, STM, and theoretical investigations. Our results strongly suggest that pyrrole adsorbs dissociatively on Si(111)-(7×7) through the breakage of N–H bond, resulting in the pyrrolyl group bonded to an adatom and the H atom bonded to an adjacent rest atom.

II. EXPERIMENTAL AND THEORETICAL CALCULATION

Experiments were performed in two ultrahigh vacuum (UHV) chambers. One of them is equipped with a high-resolution electron energy loss spectrometer (LK-2000-14R)

[a)]Author to whom correspondence should be addressed. Electronic mail: chmxugq@nus.edu.sg
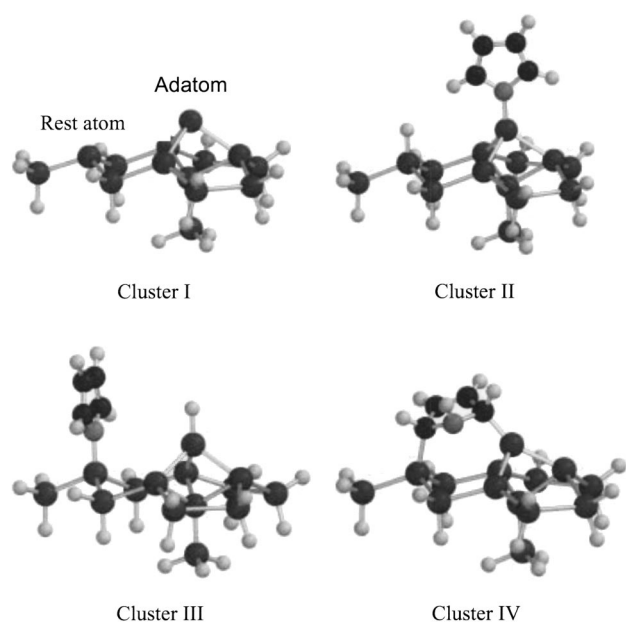
FIG. 1. Schematic illustrations of cluster I ($Si_{14}H_{18}$) and three clusters modeling possible pyrrole adsorption configurations on Si(111)-(7×7).

FIG. 2. Thermal desorption spectra of pyrrole ($m/e=67$), and fragments, hydrogen ($m/e=2$) and HCN ($m/e=27$) from multilayer pyrrole-covered Si(111)-(7×7).

for HREELS studies and a quadruple mass spectrometer (QMS) (UTI-100) for TDS and gas analysis. For HREELS measurements, a primary electron beam with an energy, E_p, of 5.0 eV impinges on the surface at an incident angle θ_i of 60° from the surface normal. The energy resolution of the spectrometer (full width at half maximum, FWHM) is determined to be ~5 meV. The spectra were taken at specular and off-specular directions, where the angle of off-specular detection refers to $\theta_{(\text{analyzer})} - \theta_{(\text{specular})}$. During TDS measurements, the ionizer of QMS is enclosed in a glass envelope with an aperture of 4 mm diameter located about 2 mm from the sample surface. The linear heating rate of 2 K/s is achieved using an RHK temperature controller.

The other chamber with a base pressure $<6 \times 10^{-11}$ Torr consists of a variable-temperature scanning tunneling microscope (Omicron Vakuum Physik GmbH) and a quadruple mass spectrometer (PPT-200EM, MKS Instruments, Inc.) for gas analysis. Constant current topographic images were acquired with a sample bias voltage in the range of -3 to $+3$ V and a tunneling current set point at the order of 0.1 nA. The (7×7) reconstructed surface can be routinely achieved by a thermal annealing method.[23]

Pyrrole (ca. 99%) was purchased from Aldrich. Prior to use, it was further purified by freeze–pump–thaw cycles and its purity was verified with MS. Pyrrole was introduced into the UHV chambers via a direct doser with a 6 mm opening at its front. During dosing, the doser is located about 1 cm from the sample surface. The exposure was measured using a B-A gauge without ion gauge sensitivity calibration.

Theoretical calculation was performed with cluster models. Clusters with suitable sizes representing only a fraction of the (7×7) unit cell were constructed and employed. Cluster I ($Si_{14}H_{18}$) (Fig. 1) was cut from the central part of MMFF94[24] optimized cluster, where the precision of atomic positions suffers the least from boundary effects. It contains
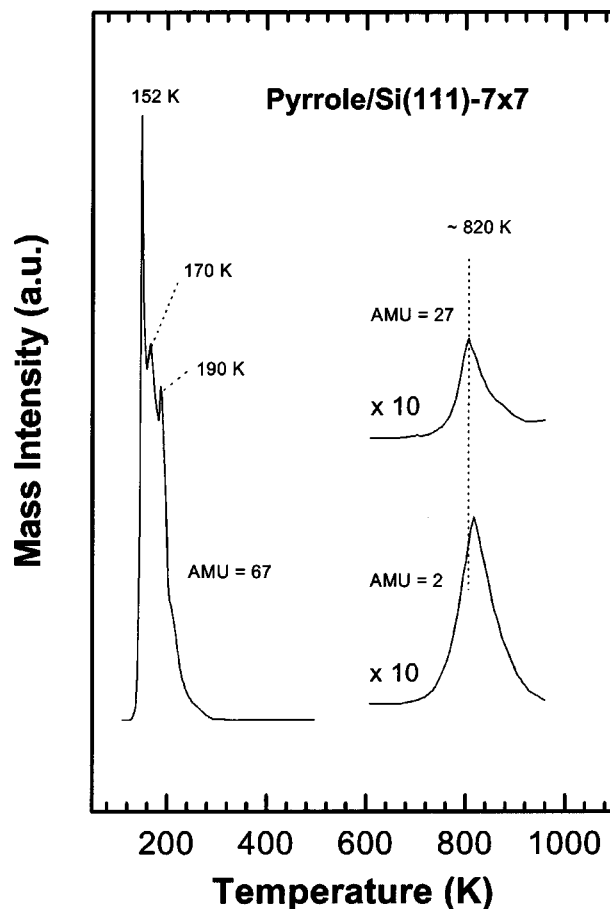
a corner adatom and an adjacent rest atom from an unfaulted subunit, which serves as a ''di-radical'' binding site for the simultaneous attachment of a pyrrolyl radical and a hydrogen atom. All capping H atoms were kept frozen during geometry optimization processes. Three possible adsorption configurations were considered (Fig. 1). One of them is the state with C_4H_4N radical attached to an adatom via the formation of Si–N linkage and H atom bonded to an adjacent rest atom (cluster II). The alternative binding configuration with pyrrolyl linked to the rest atom and H atom to the adatom is also considered (cluster III). In addition, the di-σ binding configuration formed via the two α–C atoms of pyrrole to an adatom–rest atom pair was also modeled (cluster IV), similar to thiophene adsorption on Si(111)-(7×7).[18]

Calculations were performed using SPARTAN package (version 5.1).[25] Total energies of free pyrrole molecules and clusters I–IV were calculated with both semiempirical PM3 method[26] and density functional theory (DFT) using perturbative Becke–Perdew functional (pBP86) in conjunction with a basis set DN** (comparable to 6-31G**).[25] The heat of adsorption quoted here is obtained by subtracting the total energy of the adsorbate/substrate complex from the energy sum of the substrate and gaseous pyrrole.
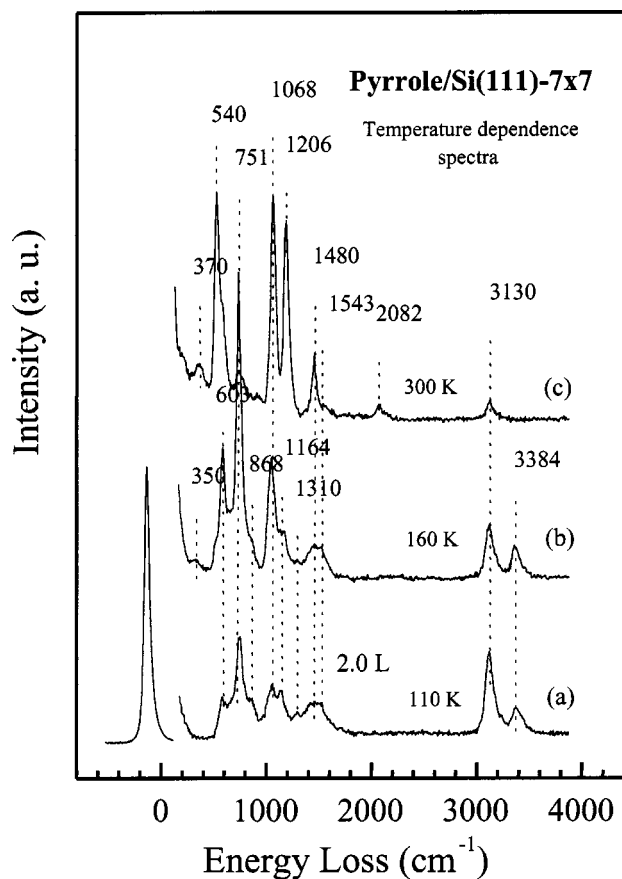
FIG. 3. Temperature dependence of HREELS spectra obtained after exposing 2.0 L of pyrrole at on Si(111)-(7×7) at 110 K (a) and subsequent annealing the surface to 160 K (b) and 300 K (c).

TABLE I. Vibrational modes assignment for pyrrole physisorbed and chemisorbed on Si(111)-(7×7) surfaces and vapor pyrrole (the vibration frequencies are given in cm^{-1}).

Vibration mode and symmetry type	Vapor phase IR frequencies	Multilayer pyrrole on Si(111)-(7×7)	Monolayer pyrrole on Si(111)-(7×7)
δ(Si–N)	···	···	370
ν(Si–N)	···	···	540
γ(N–H) B_2	565	603	···
γ(C–H) B_2	768	751	751
δ(ring) B_1	869	868	868
δ(C–H) A_1	1047	1068	1068
	···	···	1206
δ(C–H) B_1	1076	···	···
δ(N–H) B_1	1046	1164	···
	1290	1310	···
ν(ring) A_1	1380	···	···
	1418	···	···
ν(ring) B_1	1466	1480	1480
	1531	1543	1543
ν(Si–H)	···	···	2082
ν(C–H) A_1	3133	3130	3130
ν(N–H) A_1	3400	3384	···

III. RESULTS AND DISCUSSIONS

A. Thermal desorption and vibration studies

The thermal desorption spectra of pyrrole and its fragments obtained after exposing 2 L (1 L=1×10^{-6} torr·s) to Si(111)-(7×7) at 110 K are shown in Fig. 2. Molecular desorption of pyrrole ($m/e=67$) occurs in the low temperature range of 150–190 K. Three desorption peaks at 152, 170, and 190 K can be resolved and attributed to physisorbed multilayer pyrrole on the surface. In addition, hydrogen ($m/e=2$) and HCN ($m/e=27$) desorption intensities are detected at 820 K. These observations imply that the chemisorbed pyrrole does not desorb molecularly. It either dissociates on the surface or decomposes upon thermal annealing during the TDS process.

The HREELS spectra were taken after annealing the surface exposed to 2.0 L of pyrrole at 110 K to various temperatures, which are shown in Fig. 3. On a multilayer pyrrole-covered surface at 110 K, loss features are readily identified at 603, 751, 868, 1068, 1164, 1310, 1480, 1543, 3130, and 3384 cm^{-1}. These loss peaks are comparable with the vibration structures of gaseous pyrrole[27] within ca. 20 cm^{-1}. The peaks at 3130 and 3384 cm^{-1} are assigned to C–H and N–H stretching modes, respectively. The losses at 1310, 1480, and 1543 cm^{-1} are associated with the vibration modes of the heterocyclic ring. The peaks at 1164, 868, and 1068 cm^{-1} are attributable to the in-plane bending modes of N–H, ring, and

C–H, respectively. The features at 603 and 751 cm^{-1} are related to N–H and C–H out-of-plane bending modes. The detailed assignments for physisorbed and chemisorbed pyrrole on the surface, together with the IR data of gaseous pyrrole,[27] are summarized in Table I. The presence of physisorbed pyrrole at 110 K is clearly demonstrated by the good correspondence between our HREELS results and the vibrational energies of gaseous pyrrole, which is consistent with our TDS observation.

Upon thermal annealing to 300 K, all the physisorbed pyrrole desorbs from the surface, and only chemisorbed species are left. New vibrational features at 370, 540, 1206, and 2082 cm^{-1} can be clearly resolved [Fig. 2(c)]. From the spectrum, it is evident that the N–H stretching at 3384 cm^{-1} observed for physisorbed molecule is absent. However, the vibrational modes related to the ring and C–H are preserved. The assignments for the HREELS spectrum of chemisorbed species are summarized in Table I. The two vibrational features at 370 and 540 cm^{-1} are attributed to the Si–N bending and stretching, respectively. Furthermore, the 2082 cm^{-1} loss is assigned to the Si–H stretching. The detection of these new features, together with the disappearance of the 3384 cm^{-1} N–H stretching peak, clearly suggests that pyrrole chemisorbs dissociatively on Si(111)-(7×7) with the N–H bond cleavage. The fragments, pyrrolyl radical and hydrogen atom, bind to surface Si atoms, forming new N–Si and H–Si linkages.

The recent theoretical calculation on N–H and C–H bond dissociation energies (BDE) in pyrrole molecules shows that N–H BDE (~89 kcal/mol) is significantly lower than the value of ~118 kcal/mol for C–H.[28] This result implies that N–H of pyrrole may be more susceptible to dissociation upon interacting with the surface compared to the C–H bond, which is consistent with our current experimental findings.

B. Theoretical calculation

The large dimension and complexity of the (7×7) re-constructed unit cell make the accurate theoretical simulation intrinsically difficult. We performed semiempirical PM3 and DFT calculations with limited cluster sizes (Fig. 1). It is understood that the calculation may not be able to give accurate absolute values of adsorption energy. However, the difference in the adsorption energies between different configurations provides qualitative information about the thermodynamically preferred state.

PM3 calculations show that the binding energies for clusters II, III, and IV (Fig. 1) are 71.3, 66.0, and 51.0 kcal/mol, respectively. Only a small energy separation (5.3 kcal/mol) is found for the two dissociative adsorption states (clusters II and III). However, the associative adsorption via $[4 + 2]$ cycloaddition (cluster IV) has an energy substantially smaller than the dissociative reaction channels (clusters II and III) by 20.3 and 15.0 kcal/mol, respectively.

Similar trend is also predicted by the more accurate DFT calculations. The corresponding binding energies for clusters II, III, and IV are found to be 46.9, 40.2 and 16.1 kcal/mol. The energy difference (6.7 kcal/mol) between clusters II and III by DFT is comparable to the value (5.3 kcal/mol) obtained in PM3 calculation. However, their relative thermal stability over cluster IV is enhanced, evidenced in the greater energy separations (30.8 and 24.1 kcal/mol) between clusters II/III and cluster IV. Apart from the discrepancies in the absolute energy values, both calculations consistently indicate that the dissociative adsorption represented by cluster II is thermodynamically most stable.

These results are rather reasonable if considering the retention of aromaticity of pyrrole ring in dissociative adsorption in contrast to the associative $[4 + 2]$ cycloaddition. In addition, the surface intermediates formed by the dissociative adsorption are strain-free, partially contributing to the large binding energy. On the other hand, the associative adsorption state ($[4 + 2]$ cycloaddition) breaks the aromaticity and one of the double bonds. Due to the physical mismatch between the size of pyrrole ring and the adatom–rest-atom distance, such binding state is expected to be highly strained. Within the two dissociative adsorption states considered, cluster II with pyrrolyl binding on adatom is sterically more favorable compared to attaching pyrrolyl to a low-lying rest atom, where the ring may experience some repulsive interaction with the neighboring adatoms.

C. Scanning tunneling microscopic study

STM images were obtained after pyrrole adsorption on Si(111)-(7×7) at room temperature. The surface coverage presented here refers to the percentage of adatoms (the topmost atomic layer) bonded with adsorbates, which can be directly obtained by STM studies.

Figure 4 presents a topographic image (unoccupied state image) of Si(111)-(7×7) after 0.005 L exposure of pyrrole at room temperature as well as line profiles of reacted and unreacted adatoms. Although the (7×7) reconstruction is largely preserved, the adsorption of pyrrole molecules causes some adatoms to become darkened, attributable to the satu-
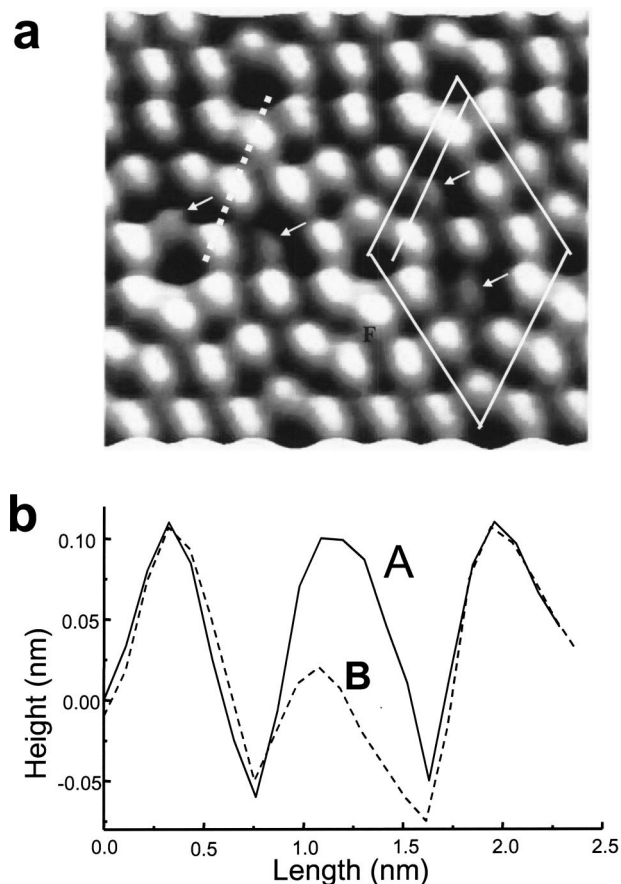

FIG. 4. (a) Empty-state image $(7.0 \times 6.7 \text{ nm})$ obtained after 0.005 L exposure at RT with a sample bias of 1.47 V and a tunneling current set point of 0.16 nA. (b) Line profiles from (a). Curve (A) corresponds to the unreacted adatom and curve (B) to the reacted center adatom.

ration of their dangling bonds (dbs) by covalent bonding with the adsorbates. The height (ca. 0.046 nm) of the reacted adatoms is found to be lower than that of unreacted adatoms (ca. 0.086 nm). Similar observations were reported for a number of molecules on Si(111)-(7×7), including H_2S/D_2S,[29] NO,[30] C_2H_2,[31] C_2H_4,[32] NH_3,[33] H_2O,[34] and O_2.[35] Careful examination of Fig. 4(b) reveals that the profile for the reacted adatom seems to be asymmetric, showing a slight distortion of the (7×7) unit cell. In fact, this result may imply the participation of an adjacent rest atom in the surface reaction. It is known that the H atom bonded to an adatom of Si(111)-(7×7) has a distinct feature, appearing like a missing adatom.[36] Thus, the darkened adatom sites observed at small coverages in our experiment are due to the binding of pyrrolyl radicals, not H atoms. The formation of Si–N linkage through pyrrolyl binding on the adatoms saturates the dangling bonds, reducing the electron density of these adatoms. This is consistent with the observed depression of reacted adatoms. The fact of not directly observing the adsorbed pyrrolyl in our STM indicates that the LUMO (lowest unoccupied molecular orbital) and HOMO (highest occupied molecular orbital) of pyrrolyl species are not close to Fermi level, E_F.

Since the rest atom is characterized by a filled dangling bond state at ~0.8 eV below Fermi level,[37] it is possible to
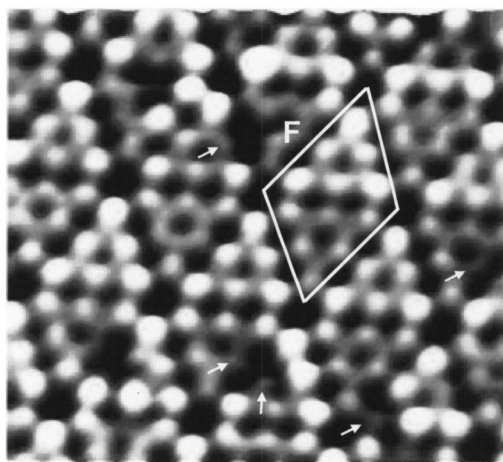
FIG. 5. Filled state image was obtained after 0.005 L at RT with a sample bias of −1.47 V and a current set point of 0.16 nA. The imaging area is 10.0×9.7 nm and the arrows show some reacted adatoms.
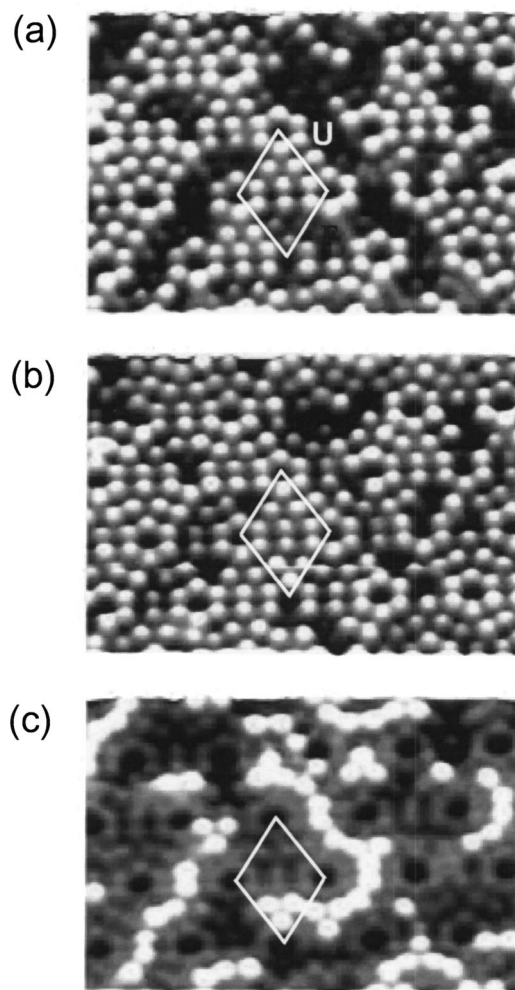

FIG. 6. Empty state images obtained after 0.05 L exposure at RT with a current set point of 0.17 nA, but different positive sample biases, (a) 2.0 V; (b) 2.5 V; and (c) 3.2 V.

image rest atoms at this bias condition. Figure 5 shows the image of occupied states upon the same pyrrole exposure at room temperature. The white arrows indicate some reacted adatoms. It is noted that the brightness or intensity of the rest atoms neighboring to reacted adatoms is significantly reduced compared to clean rest atom sites, indicating their participation in surface reaction. The involvement of rest atoms in surface reaction leads to a redistribution of dangling bond electrons, subsequently changing its image intensity. From filled-state images, the adsorption of H atom on a rest atom site was found to enhance the brightness of the three neighboring unreacted adatoms, not seen in the empty-state images.[38] In our work, one adatom adjacent to the reacted rest atom is darkened upon reaction. The remaining two unreacted adatoms indeed become brighter. This observation further indicates that H atom binds to the rest atom in the dissociative adsorption of pyrrole, agreeing well with the recent theoretical calculation.[39]

In order to gain information about higher-lying unoccupied states, a series of images of the same sample area after 0.05 L pyrrole exposure at RT was taken at higher positive sample bias voltages, shown in Fig. 6. As when increasing the sample bias to about 2.5 V, the reacted adatom sites that appear to be dark at less than 2 V become visible again, and almost keep the same height as unreacted adatoms. Since these topographic images were obtained in the CCT mode, the size and height of these reacted adatoms reflect the local density of states (LDOS) of adsorbate–Si–adatom complex in the interval $E_F - eV_{bias}$.[33] This observation suggests that the contribution of LUMO of pyrrolyl radical offsets the reduction in the LDOS of reacted adatoms upon chemisorption. When increasing the voltage to 3.2 V, the reacted adatoms become bigger in size and even more protrusive than those unreacted adatoms. This result clearly demonstrates the greater contribution of the density of unoccupied states of pyrrolyl radicals with the increase of sample bias. A similar dependence of reacted adatom intensity on bias voltage was also observed in experiments of C_2H_4,[32] NH_3,[33] SiH_2Cl_2,[40] and tetra-ethoxy-silane (TEOS)[41] adsorption on Si(111)-(7

×7). The round-shaped protruding complex observed possibly implies that the transient LDOS of reaction products cannot be obtained in our STM measurement due to the fast rotational motion of adsorbates. Based on our STM results, the possible position of LUMO of pyrrolyl radical is estimated to be about 2.3 eV below the vacuum level (4.8–2.5 eV).

In order to further understand the reaction selectivity on surface reactive sites, a detailed analysis of the spatial distribution of reacted adatoms was carried out. Table II shows the percentages of different reacted adatoms after various pyrrole exposures at RT. At 0.005 L, about 4.2% of adatoms are

TABLE II. The percentages of different reacted adatom sites and coverage under different exposures of pyrrole vapor at RT.

Exposure (L)	Fce	Fco	Uce	Uco	Coverage
0.005	59.2%	10.5%	26.3%	4.0%	4.2%
0.01	53.0%	10.3%	31.1%	5.6%	10%
0.05	44.4%	10.2%	38.0%	7.4%	21%
0.5	40.7%	14.3%	31.7%	13.3%	30%

reacted (about 1 reacted adatom/2 unit cells). Among these reacted adatoms, 59.2% are the faulted center adatom sites, 26.3% the unfaulted center adatom sites, 10.5% the faulted corner adatom sites, and 4.0% the unfaulted corner adatom sites. The ratio of reacted faulted (unfaulted) center adatoms to reacted faulted (unfaulted) corner adatoms is 5.6 (6.6). It is also noted that the total number of reacted adatoms in the faulted half is about 5.9 times of that in the unfaulted half. A high pyrrole exposure of 0.5 L results in significant increase in the surface coverage, about 30% of all adatoms reacted. At this coverage, the ratios of reacted center adatoms to corner adatoms in the faulted and unfaulted halves decrease to 2.8 and 2.4, respectively. In addition, the ratio of reacted faulted adatoms to reacted unfaulted adatoms becomes 2.6. From these experimental data, we find that the dissociative adsorption of pyrrole prefers center adatoms over corner adatoms in one subunit, and favors the faulted half compared to the unfaulted half within one unit cell. Close examination of individual unit cell of the surface after different pyrrole exposures shows that no more than three darkened adatoms within one half unit cell (faulted or unfaulted) can be found. This implies that the surface reaction is limited by the availability of adjacent adatom–rest-atom pair, consistent with the binding configuration evidenced in our HREELS and theoretical studies.

Apart from the site selectivity, the chain-like features were clearly observed in our STM images (Fig. 6). Similar structures have also been reported in the studies of H_2O adsorption on Si(100),[42] CO on Cu(110),[43] and H_2S dissociative adsorption on the Si(111)-(7×7) surfaces.[29] The formation of chainlike or cluster patterns can be attributed to the existence of attractive interaction between the neighboring adsorbates (dipole–dipole and/or electrostatic interaction). The fact that the size and length of clusters/chains do not grow further after adsorption indicates the occurrence of attractive interaction in the adsorption process, not in the final state of adsorption. It is possible that the pyrrolyl radial binding to a center adatom may attract the incoming pyrrole molecule (with a dipole moment of 1.58 debye[44]) to a nearest neighboring center adatom.

Careful statistical analysis of the spatial distribution of reacted adatoms (at exposure of 0.5 L) further confirms the presence of this interaction. In the 213 unit cells examined, 312 of faulted center adatoms (49% of all 213×3 faulted center adatoms), 243 (38%) of unfaulted center adatoms, 110 (17%) of faulted corner adatoms, and 102 (16%) of unfaulted corner adatoms are bonded with adsorbates. Each faulted center adatom has exactly one nearest neighboring unfaulted center adatoms. Therefore, if there were no interactions during the adsorption process, we would expect about 119 (243×49%) reacted center adatoms in the unfaulted halves to have neighboring reacted center adatoms in faulted halves. However, our experimentally found value is 172, clearly demonstrating the existence of attractive interaction in the adsorption process.

To further understand the difference in reactivity between the faulted and unfaulted halves within one (7×7) unit cell, the adsorption is assumed to be a mainly kinetically controlled process. Based on our statistical results, it is pos-

sible for us to estimate the difference of dissociative adsorption energy barriers between the center or corner adatoms in two different subunits by assuming the same pre-exponential factor in Arrhenius law

$$R = n_1 / n_2 = \exp(\Delta\varepsilon / kT), \quad \Delta\varepsilon = \varepsilon_2 - \varepsilon_1, \tag{1}$$

where n_1 and n_2 are the numbers of two different types of reacted adatom sites; ε_1 and ε_2, the energy barriers associated with these two different sites. We found the barrier difference between unfaulted center adatom sites and faulted center adatom sites to be 21 and 14 meV at 0.005 and 0.01 L of exposure, respectively. The values between unfaulted and faulted corner adatoms were estimated to be 25 mV at 0.005 L and 16 meV at 0.01 L. If considering nearest neighbor interaction, we could also estimate the change in energy barrier using the formula suggested by Ho *et al.*[29]

$$R = R_o(u_n / (u - u_n)) = \exp(\Delta\varepsilon / kT), \quad \Delta\varepsilon = \varepsilon - \varepsilon_n, \tag{2}$$

where u_n is the number of reacted unfaulted center adatoms with reacted neighbors in the faulted half; u, the total number of reacted unfaulted center site adsorbates; R_o, the expected ratio of the two populations. ε and ε_n are the energy barriers for reacted unfaulted center adatoms without and with reacted neighbors in the faulted half, respectively. At 30% coverage, 49% of faulted center adatoms have adsorbates, giving $R_o = (1 - 0.49)/0.49 = 1.04$. Using $u_n = 172$ and $u = 243$, we obtained an energy difference of $\Delta\varepsilon = 24$ meV, attributable to the nearest neighbor interaction between faulted and unfaulted center adatoms.

The difference in the reaction selectivity between the center and corner adatoms within one subunit of the unit cell can be related to their local electronic and geometric structures. There are two neighboring rest atoms for each center adatom, but only one for a corner adatom. Therefore, the reactivity of center adatoms would be expected to be twice that of corner adatoms. Indeed, at 0.5 L exposure, the ratio between reacted center adatoms to occupied corner adatoms is close to the value of 2. However, with this geometric factor alone, it is difficult to explain the high selectivity with a ratio of 5–7 between reacted center and corner adatoms observed at low coverage (0.005L). In a (7×7) unit cell, each corner adatom has two neighboring dimers, but one dimer for every center adatom. In chemisorption, the adsorbate at a corner site may strain two neighboring dimer bonds, resulting in a lower reactivity.

The sequential STM images of adsorption states are relatively stable (figures not shown here), implying the negligible diffusion and desorption rates in the final state of chemisorption. The selectivity for the different sites observed cannot be caused by diffusion of the chemisorbed state. A mobile precursor state governing the selectivity of various surface sites may possibly exist, similar to the one found in C_6H_6 adsorption on Si(111)-(7×7) by STM.[8]

IV. CONCLUSION

The dissociative chemisorption of pyrrole molecules on Si(111)-(7×7) was investigated using HREELS, TDS, STM, and theoretical calculation. The pyrrolyl radical and H atom formed via the N–H bond cleavage are bonded to the

adjacent adatom and rest atom, respectively. Analyses of the spatial distribution of reacted adatoms show that the adsorption is highly site selective. The faulted center adatom sites are most favored, followed by unfaulted center adatom sites, faulted corner adatom sites, and unfaulted corner adatom sites. The attractive interaction between the adsorbed pyrrolyl and the incoming pyrrole molecule in the initial adsorption process is clearly evidenced in the formation of chain-shaped STM features.

ACKNOWLEDGMENTS

[1] C. J. Baddeley, C. Hardacre, R. M. Ormerod, and R. M. Lambert, Surf. Sci. **369**, 1 (1996).
[2] D. N. Futaba and S. Chiang, J. Vac. Sci. Technol. A **15**, 1295 (1997).
[3] F. P. Netzer, E. Bertel, and A. Goldmann, Surf. Sci. **199**, 87 (1988).
[4] G. R. Schoofs and J. B. Benziger, Surf. Sci. **192**, 373 (1987).
[5] B. A. Serton, Surf. Sci. **163**, 99 (1985).
[6] G. Tourillan, S. Raaen, T. A. Skotheim, M. Sagurton, R. Garrett, and G. P. Williams, Surf. Sci. **184**, L345 (1987).
[7] C. D. MacPherson and K. T. Leung, Phys. Rev. B **51**, 17995 (1995).
[8] C. D. MacPherson, D. Q. Hu, and K. T. Leung, Surf. Sci. **276**, 156 (1992).
[9] D. Q. Hu, C. D. MacPherson, and K. T. Leung, Surf. Sci. **273**, 21 (1992).
[10] C. D. MacPherson and K. T. Leung, Surf. Sci. **324**, 202 (1995).
[11] S. Letarte, A. Adnot, and D. Roy, Surf. Sci. **448**, 212 (2000).
[12] H. D. Jeong, Y. S. Lee, and S. Kim, J. Chem. Phys. **105**, 5200 (1996).
[13] R. A. Wolkow and D. J. Moffatt, J. Chem. Phys. **103**, 10696 (1995).
[14] D. E. Brown, D. J. Moffatt, and R. A. Wolkow, Science **279**, 542 (1998).
[15] M. N. Piancastelli, M. K. Kelly, G. Margaritondo, D. J. Frankel, and G. J. Japeyre, Phys. Rev. B **34**, 3988 (1986).
[16] S. N. Patitsas, G. P. Lopinski, O. Hul'ko, D. J. Moffatt, and R. A. Wolkow, Surf. Sci. **457**, L425 (2000).
[17] R. A. Wolkow, Annu. Rev. Phys. Chem. **50**, 413 (1999), and references cited therein.
[18] Y. Cao, K. S. Yong, Z. Q. Wang, W. S. Chin, Y. H. Lai, J. F. Deng, and G. Q. Xu, J. Am. Chem. Soc. **122**, 1812 (2000).
[19] Y. Cao, Z. H. Wang, J. F. Deng, and G. Q. Xu, Angew. Chem., Int. Ed. Engl. **39**, 2740 (2000).
[20] H. S. Nalwa, *Handbook of Organic Conductive Molecules and Polymers* (Wiley, New York, 1997).
[21] I. E. Vermeir, N. Y. Kim, and P. E. Laibinis, Appl. Phys. Lett. **74**, 3860 (1999).
[22] Y. Onganer, M. Saglam, A. Turut, H. Efeoglu, and S. Tuzemen, Solid-State Electron. **39**, 677 (1996).
[23] J. A. Kubby and J. J. Boland, Surf. Sci. Rep. **26**, 61 (1996).
[24] T. A. Halgren, J. Comput. Chem. **17**, 490 (1996).
[25] W. J. Hehre, J. Yu, P. E. Klunzinger, L. Lou, *A Brief Guide to Molecular Mechanics and Quantum Chemical Calculations* (Wavefunction, Inc., Irvine, CA, 1998). See also http://www.wavefun.com/
[26] J. J. P. Stewart, J. Comput. Chem. **19**, 209 (1989).
[27] R. C. Lord and F. A. Miller, J. Chem. Phys. **10**, 328 (1942).
[28] C. Barckholtz, T. A. Barckholtz, and C. M. Hadad, J. Am. Chem. Soc. **121**, 491 (1999).
[29] M. A. Rezaei, B. C. Stipe, and W. Ho, J. Phys. Chem. B **102**, 10941 (1998); J. Chem. Phys. **109**, 6075 (1998).
[30] M. A. Rezaei, B. C. Stipe, and W. Ho, J. Chem. Phys. **110**, 4891 (1999).
[31] J. Yoshinobu, D. Fukushi, M. Uda, E. Nomura, and M. Aono, Phys. Rev. B **46**, 9520 (1992).
[32] M. N. Piancastelli, N. Motta, A. Sgarlata, A. Balzarotti, and M. De Crescenzi, Phys. Rev. B **48**, 17892 (1993).
[33] F. Bozso and Ph. Avouris, Phys. Rev. B **38**, 3937 (1988).
[34] Ph. Avouris and I. W. Lyo, Surf. Sci. **242**, 1 (1991).
[35] R. Martel, Ph. Avouris, and I. W. Lyo, Science **272**, 385 (1996).
[36] J. J. Boland, Surf. Sci. **244**, 1 (1991).
[37] R. J. Hamers, R. M. Tromp, and J. E. Demuth, Phys. Rev. Lett. **56**, 1972 (1986).
[38] R. L. Lo, M. S. Ho, I. S. Hwang, and T. T. Tsong, Phys. Rev. B **58**, 9867 (1998).
[39] A. Vittadini and A. Selloni, Phys. Rev. Lett. **75**, 4756 (1995).
[40] T. Komura, S. Okano, K. Morikawa, T. Hanada, M. Yoshimura, and T. Yao, Appl. Surf. Sci. **23**, 132 (1998).
[41] J. Spitzmuller, J. Braun, H. Rauscher, and R. J. Behm, Surf. Sci. **400**, 356 (1998).
[42] M. Chander, Y. Z. Li, J. C. Patrin, and J. H. Weaver, Phys. Rev. B **48**, 2493 (1993).
[43] B. G. Briner, M. Doering, H. P. Rust, and A. M. Bradshaw, Science **278**, 257 (1997).
[44] T. Eicher and S. Hauptmann, *The Chemistry of Heterocycles, Structure, Reactions, Sytheses and Applications* (Thieme, New York, 1995), p. 87.